Examination of the reliability of x-ray techniques for determining hydrogen-induced volume changes

G. K. Pálsson, A. R. Rennie, and B. Hjörvarsson*
Department of Physics, Uppsala University, Box 530, S-751 21 Uppsala, Sweden
(Received 15 July 2008; published 29 September 2008)

The Bragg peaks in x-ray diffraction experiments are generally taken to be a reliable measure of the average lattice distance in crystals. We show that this assumption can be misleading when determining hydrogen-induced volume changes. Experiments based on simultaneous determination of the position of the Bragg peak and the sample volume of an Fe/V(001) superlattice while expanding the lattice by *in situ* hydrogen loading serve as an illustration of this counter-intuitive effect.

DOI: 10.1103/PhysRevB.78.104118 PACS number(s): 68.55.Ln, 61.05.cm, 61.05.cp, 68.65.Cd

I. INTRODUCTION

Understanding the structural changes that arise on absorption of hydrogen is crucial for both basic research and in the development of potential applications of materials that range from hydrogen storage to the modification of magnetic and optical properties.[1–5] The structure as well as the hydrogen-induced volume changes are frequently determined using x-ray diffraction (XRD) techniques. These are often referred to as expansion coefficients and are listed in many comprehensive reviews and reference books.[6] Changes in volume are of special importance when addressing hydrogen-hydrogen interactions, phase transitions, hydrogen embrittlement, self-trapping, and thereby the rate of diffusion.[7] Changes in diffraction peak positions have also been used to determine the hydrogen concentration, from which phase diagrams have been constructed.[8,9] All these types of analysis assume that the volume changes scale linearly with the hydrogen concentration.

Several authors have reported anomalous changes in lattice parameters during hydrogen loading both in bulk samples[10] and in thin films.[11–13] While the anomalies were inferred to originate from elastic interactions with the substrate, these observations already cast doubts on the understanding of diffraction results. The investigations were carried out on films absorbing hydrogen irreversibly, hindering the separation of effects arising from irreversible and reversible lattice changes. This highlights the need to establish a consistent view on the relation between the underlying local volume changes and the observed peak shifts in XRD patterns. Investigations of this kind have been hampered by the lack of routes available to determine the volume changes, and the measured shift in XRD has often been the sole source of information on the hydrogen-induced expansion.

Here we describe an experimental approach that overcomes this problem, thus, allowing simultaneous determination of the volume changes and the shifts of the diffraction peaks. The investigation is based on x-ray analysis of an Fe/V single-crystal superlattice, which can be loaded with hydrogen reversibly and repeatedly. We observe all accessible length scales with a scattering experiment on a superlattice to determine the total thickness, chemical repetition, and atomic distances as illustrated in Fig. 1. Due to the constraining forces exerted on the film by the substrate, as well as the restoring effect of the Fe layers, the change in volume is restricted so as to be perpendicular to the surface (the z direction).[14] This allows for highly accurate determination of the changes in the observed volume and the position of the diffraction peak as will be described below.

The thickness of a single repeat, Λ, is $N\langle c\rangle$, where N is the total number of monolayers within one period and $\langle c\rangle$ is the average lattice parameter in the [001] direction. It is defined as[15]

$$\langle c\rangle \equiv \frac{\bar{n}_{\mathrm{Fe}} c_{\mathrm{Fe}} + \bar{n}_{\mathrm{V}} c_{\mathrm{V}}}{\bar{n}_{\mathrm{Fe}} + \bar{n}_{\mathrm{V}}}, \tag{1}$$

where $\bar{n}_{\mathrm{Fe}}$ and $\bar{n}_{\mathrm{V}}$ are the average number of monolayers of each material and c_{Fe} and c_{V} are the lattice parameters of each constituent in the [001] (z) direction. It should be noted that $N=\bar{n}_{\mathrm{Fe}}+\bar{n}_{\mathrm{V}}$ does not need to be an integer as it refers to an average number of atomic layers. The total thickness of the superlattice, L_s, is determined by the number of repeats, namely, $L_s=M\Lambda$. Thus, an *a priori* assumption is that for a superlattice structure, the following relation must hold:

$$L_s = M\Lambda = MN\langle c\rangle. \tag{2}$$

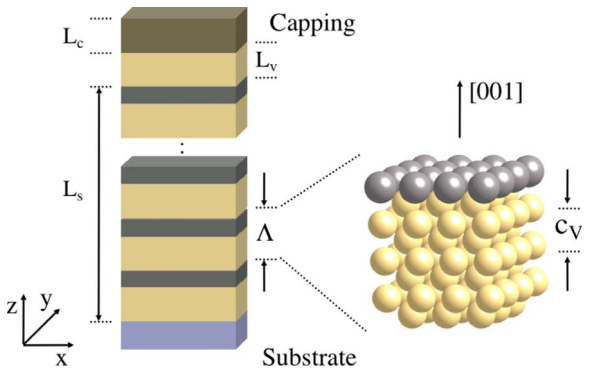

FIG. 1. (Color online) Illustration of the accessible length scales in the described experiment. The total thickness of the superlattice is denoted by L_s, the thickness of the capping layer is denoted by L_c, the lattice parameters in the [001] direction (along the z axis) are denoted by c_V and c_{Fe}, and the repeat distance for the chemical modulation is denoted by Λ.

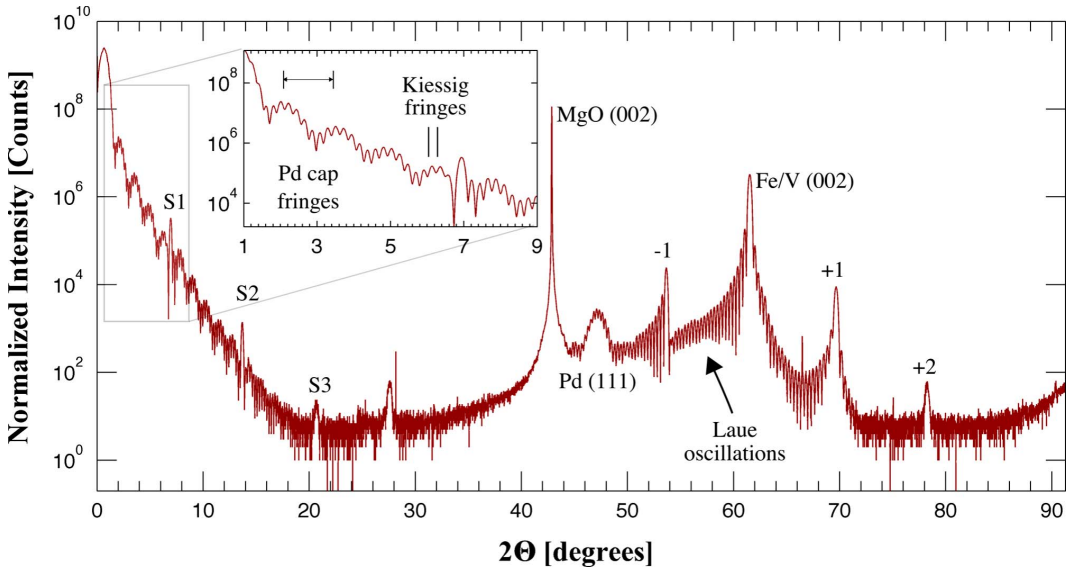

FIG. 2. (Color online) Illustration of the accessible length scales in the described experiment. The step time was roughly 1.4 s/step and the wavelength was 0.154 06 nm. For details, see text.

The relative change in the total thickness is thereby obtained easily as

$$\frac{\Delta L_s}{L_s} = \frac{\Delta \Lambda}{\Lambda} = \frac{\Delta \langle c \rangle}{\langle c \rangle}. \quad (3)$$

All the length scales should therefore give identical information on the volume changes if correctly determined.

II. EXPERIMENTAL DETAILS

A. Sample description

The sample chosen for the experiment was a single-crystal Fe/V superlattice with nominal thicknesses of the Fe and V layers, one and seven MLs (where ML stands for monolayer), respectively, and the number of repeats (M) was 25. The sample was capped with seven ML of V followed by a Pd layer with nominal thickness L_c=6.5 nm, facilitating hydrogen dissociation and protecting the sample from oxidation. The sample was grown by dc magnetron sputtering under ultrahigh vacuum (UHV) conditions on a polished single-crystal MgO (001) substrate. The epitaxial relation between the substrate and film was Fe/V (001) ∥ MgO (001) and Fe/V $[1\bar{1}0]$∥[020]. The deposition was carried out as described by Isberg *et al.*,[16] which is known to produce high-quality Fe/V structures. The rocking width (full width at half maximum) of the (002) superlattice peak was determined to be 0.06° in ω, the angle between sample and incident beam indicating low mosaicity of the sample.

In Fig. 2 we demonstrate the presence of all the length scales described in Fig. 1. These x-ray measurements were made at the W1.1 beamline of HASYLAB Hamburg, Germany at room temperature with a wavelength of 0.154 06 nm to provide an overview (at high resolution) of the entire structure of the sample without hydrogen. The rapid oscillations at angles below 18° reveal the total thickness of the sample with superimposed oscillations arising from the Pd capping. Three superlattice peaks (labeled S1, S2, and S3) are also visible in the range 0–21°. The Fe/V(002) Bragg peak is seen at 61.520(1)° and the high-angle superlattice peaks are marked by $\pm j$. Well-resolved Laue oscillations are also visible beyond the first high-angle satellites. The peak at 27° is unidentified.

The average Fe/V(002) lattice parameter in the z direction, $\langle c \rangle$, of the hydrogen-free sample was determined to be 0.3012(4) nm. The lattice parameter of bulk V is c_V^B =0.302 36(5) nm, which corresponds to a difference of 0.38%.[17] Thus, the observed (002) Bragg peak can be regarded as originating from a weakly distorted V lattice.

Before looking at the changes induced by hydrogen it is important to (i) confirm that the hydrogen-free structure is consistent with the proposed model depicted in Fig. 1 and (ii) establish that the reflectivity region gives the same results as the high-angle region. This was done in several ways. First, the positions of the superlattice peaks were determined and from them the bilayer thickness is calculated. These values for the reflectivity and the diffraction regions are summarized in the first row of Table I and are consistent within the experimental errors. Second the total thickness of the film, T, was determined by examining the Kiessig fringes in the low-angle region and the Laue oscillations in the high-angle region. Finally, the reflectivity curve was simulated using GenX,[18] which is based on Parratt's formalism[19] using the model in Fig. 1. Briefly it is a dynamic optical model that incorporates effects arising from refraction, x-ray absorption, and multiple scattering. The interfaces between the Fe and V were assumed to be sharp and the thicknesses, the density of the Fe layers, the substrate roughness, and the cap layer roughnesses were varied. The results are summarized in the third column of Table I and the fit can be seen in Fig. 3. The final row in Table I gives the total thickness of the superlattice stack including the final V layer by five different methods. It is concluded that the low and the high angles give the

TABLE I. Summary of the x-ray analysis obtained from the hydrogen-free sample (all in nm). The figures in parentheses are estimates of the 95% confidence on the last digit for each quantity.

Length scale	XRR	XRD	Sim.[a]
Λ	1.28(4)	1.287(4)	1.288(5)
L_c	6.3(1)[b]		6.3(1)
T	40.2(2)[c]		40.0(2)
L_s+L_v	33.9(3)[d],33(1)[e]	32.8(5)[f],33.5(1)[g]	33.5(1)

[a]XRR simulations using Parratt formalism.
[b]FFT of Pd fringes with refraction correction (1–7°).
[c]FFT of Kiessig fringes with refraction correction (1–7°).
[d]$T-L_c$
[e]Using S1, S2, and S3 (see Fig. 2), which yield Λ.
[f]Determined from the Laue oscillations around the (002) peak.
[g]Using Λ determined from satellites around the (002) peak.

same answer for the relevant length scales within the experimental errors.

B. *In situ* experiments

A specially designed UHV scattering chamber, allowing *in situ* exposure to hydrogen in a wide temperature and pressure ranges, was mounted on a Bruker Discover D8 X-ray diffractometer equipped with a parallel x-ray beam (CuKα_1 λ=0.154 06 nm). The sample was measured both in the low-angle reflectivity region ($2\Theta \leq 20°$) and in high angles ($2\Theta > 20°$) before and after exposure to highly purified H_2 gas at different pressures and at a constant temperature (0.1–1000 mbar). *In situ* resistance measurements were used to determine whether the dissolved hydrogen was in equilibrium with the surrounding H_2 atmosphere.[20]

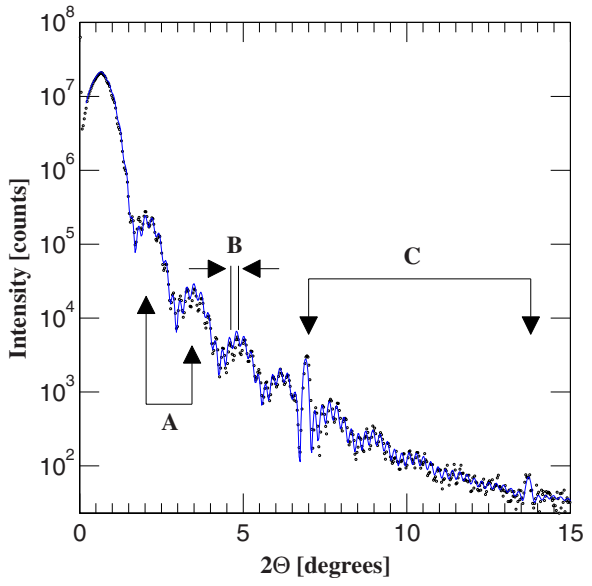

FIG. 3. (Color online) A reflectivity curve of the superlattice at 348 K and hydrogen pressure below 5×10^{-9} mbar. A shows the capping layer oscillations corresponding to L_c, B marks the total thickness oscillations corresponding to the total thickness (T), and C indicates the superlattice peaks corresponding to Λ. The step time was 5 s/step.

C. Analysis

The average lattice spacing $d_{Fe/V}$ is normally determined using Bragg's law,

$$2d_{hkl}\sin\Theta_{hkl} = \lambda, \tag{4}$$

that relates the lattice spacing d_{hkl} to the x-ray wavelength λ and scattering angle 2Θ and which (for a superlattice structure) is extended and rearranged as

$$\frac{\sin\Theta_s}{\lambda} = \frac{1}{2d_{Fe/V}} \pm \frac{s}{2\Lambda}, \tag{5}$$

where Θ_s is the angle of incidence and s is the order of the satellite. The centroid of the fundamental Bragg peak ($s=0$) corresponding to the (002) planes ($\langle c\rangle = 2d_{Fe/V}$) was determined by fitting each curve to a pseudo-Voigt function.

The determination of the shift of the Fe/V(002) peak was obtained using the MgO (002) Bragg peak from the substrate as a reference. The critical angle (around 0.66°), which depends primarily on the electron-density difference between the substrate and the vacuum, was used as a reference for determining the position of the peaks in the reflectivity region. Both the references remained unchanged during the experiment. The absorption of hydrogen changes the volume of the V layers and thereby the density, which alters the position of the total reflectivity edge. The net effect is, however, small enough to be neglected in the analysis. The bilayer thickness (Λ) can be obtained from reflectivity peaks using the kinematic approximation for superlattice structures,[21]

$$\sin^2\Theta_n = \left(\frac{\lambda}{2\Lambda}\right)^2 n^2 + 2\delta, \tag{6}$$

where n is the order of the reflectivity peak, λ is the x-ray wavelength, Θ_n is the incident angle, and δ is the deviation from unity of the refractive index for x rays. Since δ is on the order of 10^{-6} and we are looking at changes on the order of 10^{-2} in Λ, the changes in δ are also neglected. The kinematic approximation is justified as we are interested in a region where the reflectivity is low (below 10^{-3} above 7° in 2Θ). The scattering vector **Q** is perpendicular to the surface in this scattering experiment and has a length

$$Q = \frac{4\pi}{\lambda}\sin\Theta. \tag{7}$$

Λ was determined from the position of the first-order reflectivity peak ($n=1$) by removing the overall trend of decreasing reflectivity ($\approx Q^{-4}$) that arises from a sharp well-defined surface and fitting the peak using a pseudo-Voigt function.

The total thickness was determined in two ways. First, the reflectograms were simulated using the procedure mentioned in Sec. II A. Second, fast Fourier transforms (FFTs) of the reflectivity curves were made after compensating for the overall trend of decreasing reflection with an increase in Q ($\approx Q^{-4}$) mentioned in the previous paragraph as described by Bridou *et al.*[22] Since the film is thin (40 nm), the Kiessig

fringes are well defined and the FFT yields sharp peaks that are readily identified. However, the first method provides more consistent results as the FFT is sensitive to the precise range of data selected for analysis. This can arise because simple scattering theory does not apply when reflectivity is high or from effects of roughness and defects at the interfaces. The second procedure was only reliable to within about 10% and for this reason the discussion of total thickness will be based on the results of the simulations.

D. Sources of errors

Prior to discussing the experimental results, we consider the accuracy and precision of the measurements, addressing different sources of errors and how these can affect the results.

(i) *Alignment.* Before reflectometry data were collected, the height of the sample was set to the center of rotation of the diffractometer to better than 10 μm using a motorized translation stage. The definition of the origin in Θ-2Θ was determined with an accuracy, which was better than 0.001° in Θ by measurement of the attenuated direct beam. The beam on the diffractometer is repartitioned through a bent multilayer (Goebel mirror) followed by a beam compressor resulting in a parallel beam. Zero shifts (backlash) from gear systems and detector arms are minimized by always driving the motors in a single direction during final alignment and measurement.

After each change in temperature, the instrument and sample were realigned. Before alignment the instrument was allowed to reach thermal equilibrium. The height of the sample was not changed during hydrogen exposures. If the height had changed, a shift of the critical edge would have been noticed as a consequence of the resulting change in the effective zero point of the detector angle.

To determine the shifts of the Fe/V(002) diffraction peak, the MgO (002) diffraction peak was used as the reference. The accuracy of the determination of the position of the MgO peak was better than 0.001° and the precision was determined by the precision of the instrument. MgO does not absorb hydrogen and its position is therefore not changed by hydrogen exposure. Only thermal expansion contributes to the changes in this peak position. The precision of the determination of the MgO and Fe/V diffraction peak positions is therefore determined solely by the resolution of the instrument. Consequently, the accuracy in the determination of the change in the position of the Fe/V(002) peak is the same as the precision in the measurements.

(ii) *Footprint corrections.* A geometrical footprint correction was made to correct the finite length of the sample (10 mm). This correction is minor and affects only the region close to the critical edge including the first two Kiessig fringes.

(iii) *Reproducibility.* Several data points were remeasured two years after the initial experiments using the same instrument. These agreed within the experimental precision.

(iv) The resistance probe pushes down on the sample and causes it to shift in height after initial alignment. The resistance probes were therefore not moved for the duration of the experiment.

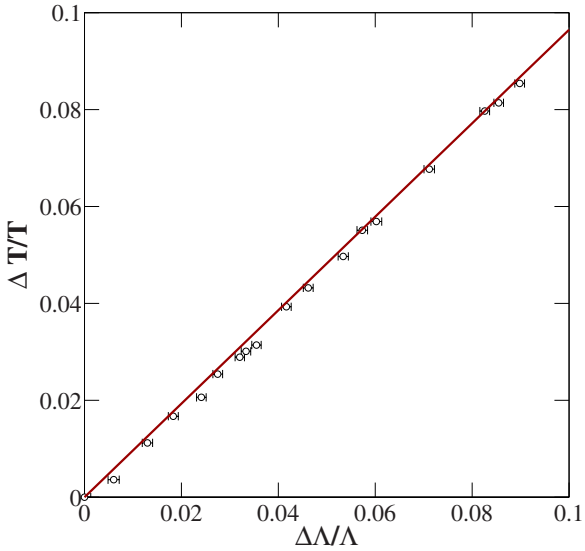

FIG. 4. (Color online) The relative changes in total thickness (T) from simulations of the data plotted versus changes in Λ. The thickness is given by $T=L_s+L_V+L_c$. The solid line is a straight-line fit through the origin with a slope of 0.96(2) with a reduced $\chi^2=1.4$.

III. RESULTS

Representative reflectivity results obtained with the *in situ* setup at 348 K and hydrogen pressure below 5×10^{-9} mbar are shown in Fig. 3. The solid line is a fit to the data as described in the sample description. The slowly varying oscillations arising from the Pd capping layer (A), Kiessig fringes (B), as well as the superlattice peaks (C), were used to determine the changes in thickness upon hydrogen absorption. The resulting changes in the total thickness (T) (as obtained from simulations of the data at different pressures) and the chemical modulation (Λ) (directly measured from peak positions) are illustrated in Fig. 4. Both the length scales give about the same change in volume upon hydrogen absorption. A linear model with the origin fixed at zero was used to fit the results using weighted linear least squares, yielding a slope of 0.96(2) at 95% confidence. The observed relative change in bilayer thickness is thus found to be reasonably consistent with the relative changes in total thickness as expected from Eq. (3) above. The determined volume change can be viewed as a direct measure of the hydrogen concentration in the sample. In the remainder of this paper we use the changes in Λ as a measure of the volume changes as Λ can uniquely be determined by simply measuring the peak position in reflectivity. We have previously established that the peak position in reflectivity gives the correct Λ and now we have shown that the changes in Λ are consistent with the changes in T.

In Fig. 5 we display diffraction results obtained under identical conditions as the reflectivity results illustrated in Fig. 3. The diffraction pattern shows the Fe/V(002) peak and the ±1 satellites. In the inset, Laue oscillations are clearly visible. The Laue oscillations correspond to the thickness of the superlattice (L_s) including the outermost V layer as discussed above. The extension of the superlattice including the final V layer was determined to be 32.8(5) nm from the Laue

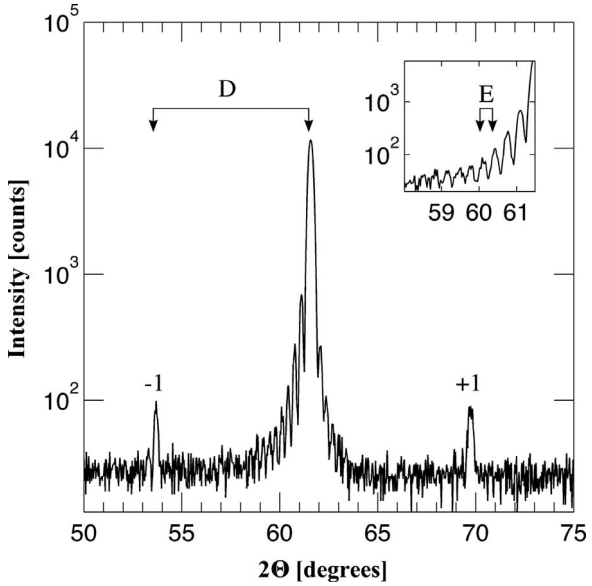

FIG. 5. An XRD pattern of the superlattice at 348 K and pressure below 5×10^{-9} mbar. D indicates the superlattice peaks corresponding to Λ and E shows the Laue oscillations corresponding to the total thickness (excluding the Pd cap). The step time was 5 s/step.

oscillations. The Pd capping does not contribute to these oscillations due to the lack of epitaxy between the superlattice stack and the Pd layer.

In Fig. 6 we display the measured changes in the spacing derived from the Fe/V(002) peak versus the volume changes determined from the changes in Λ at low Q for the sample at 348 K. As seen in the figure, there are large deviations from the expected linearity. These measurements were repeated at

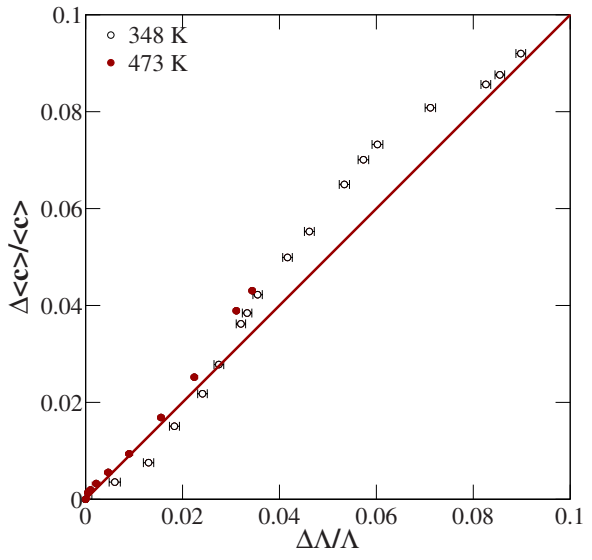

FIG. 6. (Color online) Relative changes of the Fe/V(002) peak position as a function of the relative volume changes in the sample. The data were taken at 348 K and in a pressure range of 0–739 mbar. At 473 K, the deviation at low $\Delta\Lambda/\Lambda$ vanishes. The red solid line represents the expected scaling of 1.0. The uncertainty in the vertical direction is smaller than the symbols.

different temperatures. A substantial variation in the deviations below $\Delta\Lambda/\Lambda=0.02$ was observed in the temperature range 348–493 K. A linear relation was obtained at temperatures above 473 K, with no measurable deviation. No such changes were observed in the range 0.02–0.09 in $\Delta\Lambda/\Lambda$, where the deviation from linearity was independent of temperature. Further, shifts in the satellites surrounding the main Bragg peak from the high-angle data followed the same trend as the shift in the Bragg peak itself.

IV. DISCUSSION

Before addressing the possible causes of the inconsistency in the changes in volume and the average lattice parameter, let us discuss how hydrogen is absorbed and distributed in body-centered-tetragonal superlattices such as Fe/V (001). Vanadium and iron exhibit two of the fastest hydrogen diffusion rates observed in metals (7×10^{-5} cm^2/s at 348 K for V and 1×10^{-4} cm^2/s at 348 K for Fe).[23,24] Thermodynamic equilibrium within the sample is therefore reached swiftly. The equilibrium with the surrounding H_2 gas atmosphere depends on surface conditions and was monitored by *in situ* resistivity changes and was thereby confidently assessed. The time required to reach equilibrium was on the order of tens of seconds at the lowest concentrations (low pressures) and moderate temperatures, and up to 30 min at high concentrations. The rate limiting factor during the hydrogen absorption is therefore predominantly related to the dissociation and the initial diffusion processes in the near surface region at low concentrations. At high concentrations (pressures), the increase in the equilibrium time can be related neither to surface effects nor diffusion. Configurational critical slowing down is a probable cause for this increase in equilibrium time as discussed by Olsson *et al.*[25]

The hydrogen uptake in the MgO substrate is endothermic and can be neglected in the current context. The hydrogen absorption is endothermic for Fe (+0.29 eV/H) (Ref. 26) while it is exothermic in V (−0.3 eV/H).[27] This gives rise to a variation in the hydrogen density as the hydrogen is preferably absorbed in the V layers.[28] This phenomenon is well established in superlattices with Fe layers as thin as two monolayers. The hydrogen density in the V is substantially lower at the Fe interfaces, giving rise to a concentration gradient that depends on the hydrogen concentration. When the thickness of the Fe layers is decreased, the extension of the interface region as well as the gradient in hydrogen density diminishes. The concentration modulation in the current samples is therefore relatively small as the Fe layer is only one monolayer. The modulation of the hydrogen density is still seen by the changes of the intensity of the reflectivity peaks at low scattering angles. Concentration gradients at length scales larger than Λ can be excluded as this would give rise to broadening of the reflectivity peaks.

Hydrogen occupies octahedral sites (O_z) in the superlattice structure, where the z direction is perpendicular to the sample surface as defined in Fig. 1. The (O_z) occupancy causes large local strain fields,[29] which propagate to the surface, contributing to an expansion of the sample.[30] At low concentrations there are local changes in lattice parameters

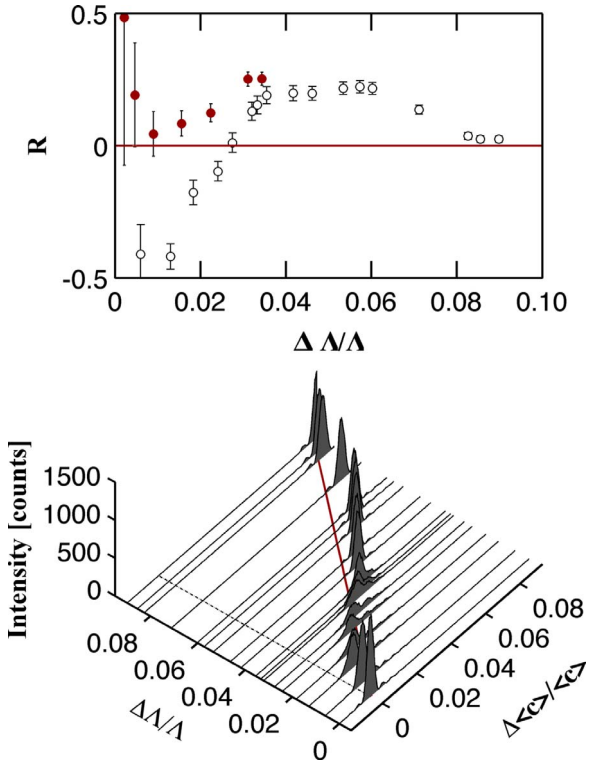

FIG. 7. (Color online) Diffraction peaks from the (002) lattice planes of the superlattice at 348 K plotted against change in the bilayer thickness Λ. The upper frame shows the normalized difference R from the expected scaling defined by Eq. (8). The solid symbols in the upper panel correspond to 473 K. The angular range is converted into lattice spacing using Eq. (5). The line in the lower frame shows the volume changes corresponding to the expected scaling of slope unity [see Eq. (3)]. The hydrogen concentration scales with the volume change and the maximum expansion corresponds to almost one hydrogen per vanadium atom $[(\mathrm{H}/V)\approx 1]$.

around dissolved hydrogen atoms ranging from 0.28 to 0.36 nm, while a fraction of the structure retains its unstrained value[29] of around 0.30 nm. If this local strain was of importance for the observed deviations in the measured lattice parameters, one would expect large changes in the intensity of the diffraction peaks while changing the hydrogen concentration.

Figure 7 shows the position and the intensity of the (002) diffraction peaks as a function of the change in thickness (Λ). To ease the comparison, the angular axis has been converted to a change in lattice spacing. It should be noted that this is not strictly correct as the width of the peak is not solely governed by a distribution of lattice parameters. Finite-size broadening as well as microstrain, if present, and instrumental broadening contribute to the width of the peak.

As seen in the figure, the integrated intensity of the (002) peak decreased to 0.2 of the initial value at $\Delta\Lambda/\Lambda\approx 0.025$. This decrease is accompanied by a broadening of the peak in 2Θ up to a volume change of $\Delta\Lambda/\Lambda\approx 0.04$. In the range $0.04\leq\Delta\Lambda/\Lambda\leq 0.09$, the intensity and the width of the peaks are close to the initial values. The transverse widths (rocking curves measured by rotating the sample only) were independent of the hydrogen content and this excludes trivial effects such as increased mosaicity of the sample as a reason for the decrease in intensity. Thus, 80% of the intensity is scattered away from the Bragg peak and should be considered as indicative of reduction in the order of the [00l] direction as found when diffuse scattering increases.

The line in Fig. 7 was drawn using Eq. (3) illustrating the previously discussed scaling of slope one. Here we define the difference from the expected scaling as

$$R=\left(\frac{\Delta\langle c\rangle}{\langle c\rangle}-\frac{\Delta\Lambda}{\Lambda}\right)\Bigg/\frac{\Delta\Lambda}{\Lambda} \tag{8}$$

and this is shown in the upper panel of Fig. 7. At low concentration (small expansion) the shift in the lattice parameter is grossly underestimated (40%). At slightly higher concentrations, corresponding to a relative volume change in the range 0.03–0.07, the shift overestimates the change in the lattice parameter. At the highest concentrations the shift in the lattice parameter approaches the expected one. There is a marked correlation that is seen between the changes in the intensity and the deviation in the shift of the Bragg peak.

At the lowest temperature, the relative deviation from the expected scaling is largest in the ranges of concentration that do not exhibit stoichiometric phases. Consider first the completely filled lattice corresponding to $[\mathrm{H}/\mathrm{V}]=1$. As all the O_z sites are occupied, the lattice has a well-defined lattice parameter. By decreasing the concentration, the vacant O_z sites will exhibit large changes in the local atomic distances.[29] If the distribution in the local strain field is responsible for the deviation in the measured lattice parameters, the difference should be absent at the highest concentration, which is consistent with our observations.

The β phase in V_2H corresponds to $\Delta\Lambda/\Lambda\approx 0.04$, using the previously determined relation between hydrogen concentration and volume changes. Every second O_z is occupied in the β phase, giving rise to well-defined local configurations with minimal variation in the local strain field. A minimum intensity is observed at $\Delta\Lambda/\Lambda\approx 0.03$, which corresponds to the crossover from negative to positive deviation in R (see Fig. 7). It is therefore plausible that the changes in intensity arise from spatial variation in the lattice spacing caused by partial ordering resembling that of the β phase. Olsson *et al.*[31] investigated the hydrogen uptake of a Fe(2 ML)/V(12 ML) (001) superlattice in the temperature range 398–473 K. A substantial temperature dependence was observed for both the enthalpy and the entropy, leading to lowering of the total energy with decreasing temperature. Since the critical temperature was determined to be 251(1) K, these changes were taking place well above the phase boundary and can therefore be seen as a signature of critical fluctuations. Thus, a conceptual framework for the temperature dependence of the deviation at the lowest concentrations becomes apparent, where we assign the changes in the scaling to the presence of critical fluctuations. This view is supported by the decreasing deviation from linearity with increasing temperature (see upper panel in Fig. 7).

Bloch *et al.*[32] observed similar changes in the intensity of the Bragg peak from a 50-nm-thick V (001) film above the deduced critical temperature [460(20) K]. When approaching the critical temperature, a clear asymmetry of the Bragg peak

is developed, indicating a distribution in the lattice parameter. Thus, although the thickness of the V layer is increased to an extent that closely mimics the bulklike properties, large effects are seen in intensity, width, and symmetry of the Bragg peak. If the reduced intensity reflects the same underlying configuration changes as assumed here, the use of the changes in the Bragg-peak position as a measure of changes in the hydrogen-induced expansion will be misleading.

We used a one-dimensional discrete lattice model to simulate the observed behavior but were unable to model the effects that are described above. This implies a need for improved simulation tools for diffraction studies of materials with distributions in the lattice spacing. This might even require full three-dimensional real-space calculations to capture the complete influence of the three-dimensional local distortion of the atomic positions on the scattered intensity. We therefore conclude that the angular position of diffraction peaks is not a good measure of volume expansion in such experiments.

V. CONCLUSION

Simplistic interpretation of x-ray diffraction results does not give a reliable measure of the hydrogen-induced volume changes. Only by probing the relevant length scales can one obtain a correct measure of the volume change. This is demonstrated here for the particular case of absorption in a superlattice. It is possible that sophisticated modeling of the diffraction pattern in terms of structure, disorder, and composition as regards peak intensity, width, and position would yield reliable information. Our interpretation of the discrepancy is not reliant on the particular geometry of a superlattice but depends rather on the presence of local strain fields, causing a distribution in lattice distances. The findings therefore have far reaching consequences for understanding and modeling the influence of local strain fields and constraints on diffraction data. The results call for review of the simple practice of determination of the volume expansion from the average lattice parameter using x-ray diffraction.

ACKNOWLEDGMENTS

This work was financially supported by the Swedish Research Council (VR) and the Knut and Alice Wallenberg foundation (KAW). We would like to thank H. Zabel for giving us the possibility to use the W1.1 beamline at HASYLAB Hamburg, Germany. A. Liebig is thanked for growing the sample.

*Author to whom correspondence should be addressed. FAX: +46(0)18-4713524.
Electronic address: bjorgvin.hjorvarsson@fysik.uu.se; http://material.fysik.uu.se/

[1] L. Schlapbach and A. Züttel, Nature (London) **414**, 353 (2001).
[2] J. N. Huiberts, R. Griessen, J. H. Rector, R. J. Wijnaarden, J. P. Dekker, D. G. de Groot, and N. J. Koeman, Nature (London) **380**, 231 (1996).
[3] F. J. A. den Broeder *et al.*, Nature (London) **394**, 656 (1998).
[4] B. Hjörvarsson, J. A. Dura, P. Isberg, T. Watanabe, T. J. Udovic, G. Andersson, and C. F. Majkrzak, Phys. Rev. Lett. **79**, 901 (1997).
[5] F. Klose, C. Rehm, D. G. Nagengast, H. Maletta, and A. Weidinger, Phys. Rev. Lett. **78**, 1150 (1997).
[6] *Hydrogen Metal Systems I*, Solid State Phenomena Vols. 49-50, edited by F. A. Lewis and A. Aladjem (Scitec, Zurich, 1996), Chap. 9, p. 401.
[7] A. M. Stoneham, Ber. Bunsenges. Phys. Chem. **76**, 816 (1972).
[8] H. Zabel and H. Peisl, Acta Metall. **28**, 589 (1980).
[9] Y. Fukai, T. Haraguchi, H. Shinomiya, and K. Mori, Scr. Mater. **46**, 679 (2002).
[10] R. Feenstra, D. de Groot, and R. Griessen, J. Less-Common Met. **104**, 43 (1984).
[11] C. Rehm, H. Maletta, M. Fieber-Erdmann, E. Holub-Krappe, and F. Klose, Phys. Rev. B **65**, 113404 (2002).
[12] H. Maletta, C. Rehm, F. Klose, M. Fieber-Erdmann, and E. Holub-Krappe, J. Magn. Magn. Mater. **240**, 475 (2002).
[13] P. F. Miceli, H. Zabel, J. A. Dura, and C. P. Flynn, J. Mater. Res. **6**, 964 (1991).
[14] G. Andersson, B. Hjörvarsson, and P. Isberg, Phys. Rev. B **55**, 1774 (1997).
[15] A. Segmuller and A. E. Blakeslee, J. Appl. Crystallogr. **6**, 19 (1973).
[16] P. Isberg, B. Hjörvarsson, R. Wäppling, E. B. Svedberg, and L. Hultman, Vacuum **48**, 483 (1997).
[17] M. E. Straumanis, J. Appl. Phys. **30**, 1965 (1959).
[18] M. Björck and G. Andersson, J. Appl. Crystallogr. **40**, 1174 (2007).
[19] L. G. Parratt, Phys. Rev. **95**, 359 (1954).
[20] S. Olsson, Ph.D. thesis, Uppsala University, 2003.
[21] B. K. Agarwall, *X-Ray Spectroscopy*, Springer Series in Optical Sciences Vol. 15 (Springer, New York, 1979).
[22] F. Bridou, J. Gautier, F. Delmotte, M. Ravet, O. Durand, and M. Modreanu, Appl. Surf. Sci. **253**, 12 (2006).
[23] *Hydrogen Metal Systems I*, Solid State Phenomena Vols. 49-50, edited by F. A. Lewis and A. Aladjem (Scitec, Zurich, 1996), Chap. 9, p. 371.
[24] K. Kiuchi and B. McLellan, Acta Metall. **31**, 961 (1983).
[25] S. Olsson, P. Blomquist, and B. Hjörvarsson, J. Phys.: Condens. Matter **13**, 1685 (2001).
[26] R. Griessen and T. Riesterer, *Hydrogen in Intermetallic Compounds I*, Topics in Applied Physics Vol. 63 (Springer, New York, 1988).
[27] H. Bleichert and H. Wenzl, Phys. Status Solidi B **144**, 361 (1987).
[28] G. Andersson, P. H. Andersson, and B. Hjörvarsson, J. Phys.: Condens. Matter **11**, 6669 (1999).
[29] T. Burkert, A. Miniotas, and B. Hjövarsson, Phys. Rev. B **63**, 125424 (2001).
[30] G. Alefeld, Ber. Bunsenges. Phys. Chem. **76**, 746 (1972).
[31] S. Olsson, A. M. Blixt, and B. Hjörvarsson, J. Phys.: Condens. Matter **17**, 2073 (2005).
[32] J. Bloch, B. Hjörvarsson, S. Olsson, and R. Brukas, Phys. Rev. B **75**, 165418 (2007).